IOP Conference Series: Earth and Environmental Science

Development of thermal image velocimetry techniques to measure the water surface velocity

Development of thermal image velocimetry techniques to measure the water surface velocity

A Saket[1], W L Peirson[1], M L Banner[2] and X Barthelemy[1,2]
[1] Water Research Laboratory, School of Civil and Environmental Engineering, UNSW Australia, 110 King Street, Manly Vale, NSW 2093, Australia
[2] School of Mathematics and Statistics, UNSW Australia, Sydney, NSW 2052, Australia

Email: a.saket@wrl.unsw.edu.au, w.peirson@unsw.edu.au, m.banner@unsw.edu.au, and x.barthelemy@wrl.unsw.edu.au

Abstract. Particle image velocimetry (PIV) is a state-of-the-art non-intrusive technique for velocity and fluid flow measurements. Due to ongoing improvements in image hardware and processing techniques, the diversity of applications of the PIV method continues to increase. This study presents an accurate thermal image velocimetry (TIV) technique using a CO_2 laser source to measure the surface wave particle velocity using infrared imagery. Experiments were carried out in a 2-D wind wave flume with glass side walls for deep-water monochromatic and group waves. It was shown that the TIV technique is robust for both unforced and wind-forced group wave studies. Surface wave particles attain their highest velocity at the group crest maximum and slow down thereafter. As previously observed, each wave crest slows down as it approaches its crest maximum but this study demonstrates that the minimum crest speed coincides with maximum water velocity at the wave crest. Present results indicate that breaking is initiated once the water surface particle velocity at the wave crest exceeds a set proportion of the velocity of the slowing crest as it passes through the maximum of a wave group.

1. Introduction

Visualisation techniques play a central role in fluid mechanics in quantifying the behaviour of a flow field. One of the main non-intrusive techniques for velocity and fluid flow measurements is particle image velocimetry (PIV). Due to ongoing improvements in image hardware and processing techniques, the diversity of applications of the PIV method continues to increase. Advances in PIV techniques have led to experimental investigations of complex problems providing a foundation for development of more accurate numerical models. During the last two decades, the PIV technique has been widely used in the field of wave mechanics [1–7].

Understanding of velocities and accelerations of waves is essential for calculating forces on marine structures. For breaking waves this force is potentially much larger than for non-breaking waves. Therefore, reliable characterisation of the wave hydrodynamics particularly for breaking waves is important to improve the design of ocean and coastal structures.

A fundamental and long-standing gap in our understanding of deep-water wave breaking is how to characterise and predict the breaking onset. The kinematic breaking criterion based on surface particle and wave crest velocities is often suggested to predict the onset of breaking. The surface kinematics associated with wave breaking has been studied using a suite of imaging techniques during the last two decades [1, 8–13]. Because measuring the surface particle velocity and the defining the crest speed are difficult, evaluation of this criterion remains nontrivial.

Banner *et al*. [14] studied deep water wave kinematics numerically, both in the laboratory and the field and have shown that the dominant waves in a group systematically slow down as they pass through the group maximum by between 10 and 30%. Barthelemy *et al*. [15] show numerically that the onset of breaking occurs once the water surface particle velocity at the wave crest exceeds a set proportion of the velocity of the slowing crest as it passes through the maximum of a wave group.

This contribution presents evaluation of a thermal image velocimetry (TIV) technique to measure the surface wave velocity using infrared imagery. Experiments were carried out in a 2D wave flume with glass side walls. Hot water droplets and a CO2 laser were used to create localised thermal signatures on the water surface, which were tracked and analysed.

2. The experiment

2.1. Experimental facilities

The experiments were conducted in the two-dimensional wind-wave tank at the Water Research Laboratory used previously by Banner and Peirson [16] (figure 1). The wave tank is 30 m long, 0.6 m wide and 0.6 m high with glass side walls and was filled with water to the depth of 0.46 m. Waves were generated using a computer-controlled, flexible bottom-cantilevered wave paddle located at one end of the flume. At the other end, a flexible reticulated polyester-urethane foam absorbent beach was installed to minimise reflections of the generated waves.

A movable wind tunnel with the length of 7.5 m and the roof of 0.5 m above the still water surface was mounted on the flume. A fan installed at the downstream of the tunnel generated wind flow and an adjustable honeycomb flow provided a uniform air flow within the wind tunnel. The wind speed was measured at the centre of the tunnel approximately 4.8 m downwind of the inlet and 0.25 m above the still water level using a pre-calibrated hot probe air velocity meter (Velocicalc model 8347).

For generating wind-forced waves, wind intensity was controlled by varying the fan input voltage using a metered Variac. Paddle-generated waves under wind forcing were investigated for different wind speeds in the range of 1.0 to 2.2 m/s.

To find the paddle amplitude corresponding to the transition between maximum (non-breaking) recurrence and marginal breaking, light was projected inside the tunnel and the transitional condition was determined visually. The paddle amplitude was increased systematically until the location of initial breaking was detected.

Two linear arrays of capacitance wave probes with 200 mm wire elements were located at each side of the flume to record the water elevation using a National Instruments PCI-6225 data acquisition system at 1000 Hz sample rate per channel. The probe resolution was 0.1 mm with a linearity of ±0.2 mm over their 200 mm length. To minimise any effect of the probes on the wind flow, the wave probe signal conditioning boxes were mounted outside the tunnel, with probes connected to the boxes via 6 mm diameter cables.

Five wave probes were installed along the one side of the tank with the spacing of 60 mm to measure the crest speed. At the other side of the tank, seven wave probes with the spacing of 100 mm were installed to measure the wave length. The water level time series captured by the wave probes were interpolated in space to obtain the zero-crossing locations at the time of the wave group maximum and, thereby, the length of the crest in the direction of propagation and crest elevation. The local steepness S_c was calculated using the length of the crest in the direction of propagation and the maximum crest elevation for each wave group.

2.2. Wave conditions

To measure the wave crest speed and water particle velocity, monochromatic and group waves were generated by the paddle. The initial conditions for generating wave packets were based on Banner and Peirson [2007].

Bimodal spectrum (Class 2) and chirped (Class 3) initial wave packets were investigated in the current study. The form of the bimodal initial spectrum was taken as:

$$\eta = a_0 \cos(k_0 x) + \varepsilon a_0 \cos\left(\frac{N+1}{N} k_0 x - \frac{\pi}{18}\right) \tag{1}$$

where η is the water surface elevation, a_0 is the initial amplitude, k_0 is the wave number, N is the number of waves in the group and ε=0.1.

The chirped wave packet was taken to have the form:

$$x_p = a - 0.25 A_p \left(1 + \tanh\frac{4\omega_p t}{N\pi}\right)\left(1 - \tanh\frac{4(\omega_p t - 2N\pi)}{N\pi}\right)\sin\left(\omega_p (t - \omega_p C_{t2} t^2 / 2)\right) \tag{2}$$

where x_p represents the wave paddle motion, A_p is proportional to the piston amplitude, t is time, ω_p is the paddle angular frequency and C_{t2} is the chirp rate of the linear modulation.

3. TIV system

In this study, two TIV methods were used to measure the horizontal water particle velocities. The system consisted of heat sources, an infrared imaging camera, a computer-controlled shutter, an acoustic sensor, synchroniser and a computer controlling the system components.

3.1. Localised thermal signatures on the water surface

Initially a thermos flask was used to deposit hot water droplets on the water surface with low (<10) Weber number ($W = \varrho u^2 d/\sigma$), where ϱ is the droplet density, u is the mean droplet impact velocity, d is the droplet diameter and σ is the surface tension. The thermos was mounted at the centre line of the flume with two linear arrays of wave probes just inside each of the tank side walls on a trolley (figure 1a). To adjust the time interval between droplets and the dimension of the droplets, a valve and nozzle were installed on the thermos. For group waves, hot droplets were laid down upstream of the group maximum location.

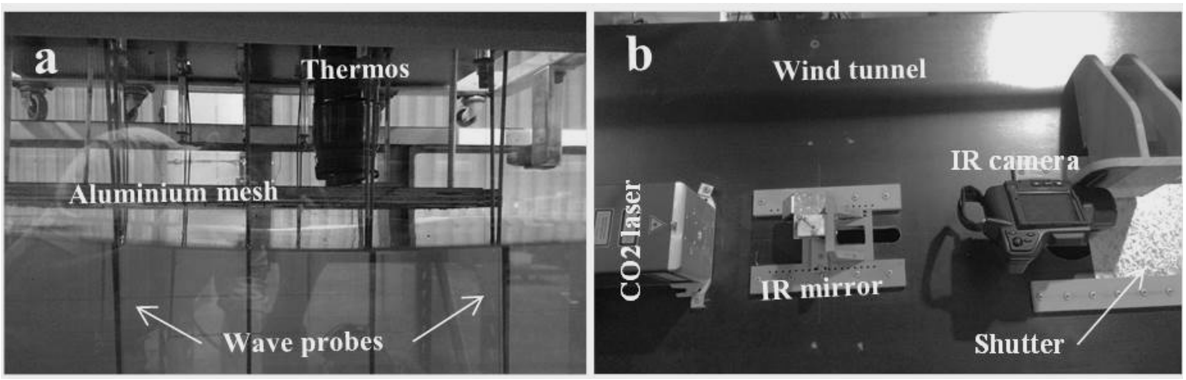

Figure 1. Laboratory deployment of instrumentation: (a) Side view showing positioning of the Thermos, wave probes and an aluminium calibration mesh installed on a trolley. (b) View from above showing the wind tunnel, CO_2 laser system, adjustable IR mirror, infrared imaging camera and computer-controlled shutter. Note that the Thermos and calibration mesh were removed once the laser system was deployed.

In order to improve the localisation of hot spot formation on the water surface, a CO_2 laser (Firestar ti100) system was developed to irradiate the water surface. The laser was mounted at the centre of the wind tunnel roof to produce heated circular patches with a diameter of approximately 4 mm upstream of the group maximum location (figure 1b).

As CO_2 lasers produce a beam of infrared light with 10.6 μm wavelength, an IR flat mirror was installed on an adjustable holder in front of the laser head to reflect the laser light on to the water surface. To minimise the diameter of the heated patches, the duty cycles were set as small as possible. The range of laser duty cycles for different wave packets was selected between 5 to 10 ms.

3.2. Infrared imaging camera
The TIV system used an infrared imaging camera (Flir T420) to acquire images of surface displacements from above, capturing 320×240 pixel images of the surface with the $25^{o}\times19^{o}$ field of view at 30 frames per second (figure 1b). The physical resolution of the thermal imager was approximately 0.66 mm per pixel at the water surface, determined using calibration grids placed within the field of view.

For the TIV system using hot water, the camera was mounted on the trolley at the centre line of the tank and central to the wave probe arrays. An aluminium mesh was installed in the field of view of the camera. To adjust the level of the grids for calibrating the images, the mesh frame was connected to the trolley using four adjustable bars. In the CO_2 system, the thermal camera was mounted at the centre of the wave probe arrays on the wind tunnel roof to observe the tank water surface through a shuttered window 3.6 m downwind of the wind tunnel inlet. Because the laser reflections could potentially damage the camera's image sensor, a computer-controlled shutter was installed beneath the camera and the shutter remained closed during surface irradiation.

3.3. Synchronisation
In the TIV system, one of the wave probes was applied as a trigger to synchronise the wave signals, laser pulses and the shutter using a National Instrument PCI-6221 data acquisition system. At a selected water surface level, laser pulsing commenced with a defined duty cycle. After surface irradiation, the shutter was opened and the thermal camera monitored the motion of the heated patches on the water surface. An acoustic sensor was installed on the shutter to synchronise the shutter motion, wave probes and camera image capture. The absolute time reference between the thermal imagery and the wave probes was ±17 ms, determined by the camera framing rate.

3.4. Experiments
To validate the technique, the present experimental study was conducted to measure the water surface particle velocities and wave crest speeds for deep-water non-breaking and breaking waves with and without wind forcing. The TIV techniques were applied for monochromatic, C2N5 and C3N7 where *C* is the wave class and *N* is the number of waves in each temporal wave packet. A Class 3 wave packet (*N*=7) was selected to analyse under wind forcing. Before starting each experiment, the water surface was cleaned by generating waves to transport all slick material along the surface of the tank water to the beach. Once the water surface had been cleaned, the wave probes were immersed in the tank for approximately 1 hour to ensure their signal stability. To determine the conditions of maximum recurrence and marginal breaking for each group, paddle amplitudes were incrementally increased. The fetches of the group maximum were found carefully and the TIV system was sited over each location for subsequent measurement of the local wave characteristics and surface current. Initially, hot water droplets were used to generate hot spots on the water surface. As the droplets lost their thermal signatures quickly, it was necessary to deposit each droplet just before arrival of the wave crest.

Subsequently, the CO_2 laser system was synchronised to apply the heated patches to the water surface. The maximum wind speed at which traceable and sufficiently-localised heat patches could be tracked on the water surface was approximately 2.0 m/s. For wind speeds between 1.5 m/s and 2.0

m/s, hot spots rapidly expanded on the surface but they were still recognisable. Heated patches on wave crests for wind speeds higher than 2.0 m/s were not easy to track as they disappeared very quickly. Therefore, the maximum wind speed used for the present study was approximately 2.0 m/s.

4. Results and discussion

The TIV system was applied to non-breaking monochromatic and group waves. The displacement of heated patches at the crest of monochromatic and Class 3 waves are shown in figure 2. The water surface velocity was determined by tracking the leading edge of the heated patch in successive video frames and the wave crest speed was measured using the array of wave probes. The average and standard deviation from five measurements of water surface velocity (U_s), wave crest speed (C), wave amplitude (a) and wave number (k) for monochromatic waves (T = 0.7 sec) has been presented in table 1. The wave parameters were measured using the two arrays of wave probes.

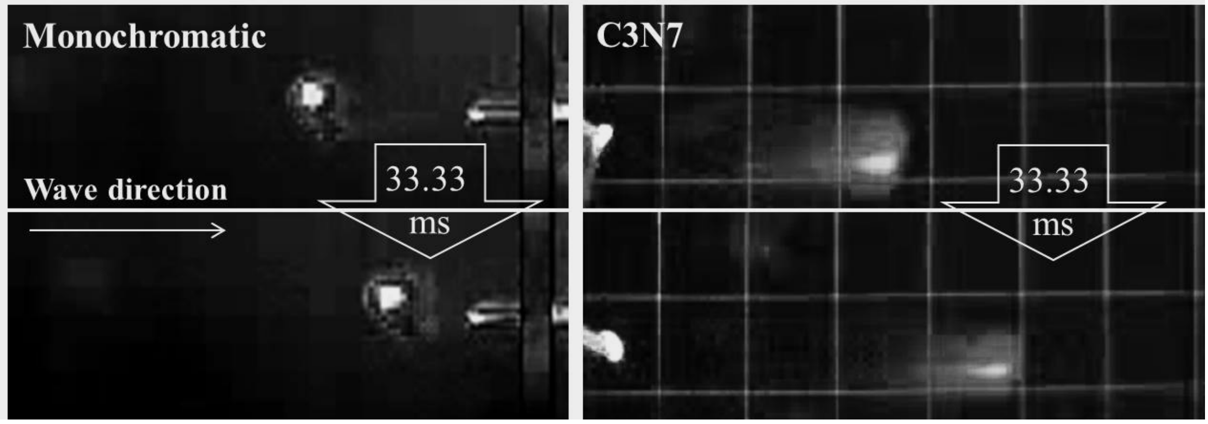

Figure 2. Tracking the hot spot on the wave crests of a monochromatic wave and a C3N7 wave packet for two successive frames using infrared imagery to measure the surface particle velocity.

The most challenging measurements required capturing crest surface velocities at the point of the group maximum. This required ensuring that the position of heat patches coincided with the crest concomitant with occurrence of the group maximum. Because the TIV method using the Thermos was not able to synchronise the droplets with the wave probes, it was not possible to have a precise measurement of the crest surface velocities for grouped waves. In addition, the experiment was conducted for breaking waves and it was found that the hot spots disappeared quickly and it was not possible to track those spots on the water surface. For wind-forced waves, the hot droplets were not trackable as they had lost their heat before reaching the water surface.

Table 1. The results of wave crest speed (C), wave amplitude (a), wave number (k), and water surface velocity (U_s) for a single case of monochromatic non-breaking waves (T = 0.7 s).

	C (m/s)	a (m)	k (m^{-1})	$a.k.C$	U_s (m/s)
Average	1.12	0.0092	7.84	0.081	0.085
Standard Deviation	0.014	0.00005	0.02	0.001	0.002

The TIV technique using the CO_2 laser improved the technique significantly for both breaking waves and wind-forced waves. Nonetheless, trial and error iteration was required to ensure that the position of heat patches coincided with a crest maximum event. The heated patches produced by the laser remained on the water surface longer than the droplets and were much more compact (approximately 4 mm in diameter). This allowed us to measure the water surface velocities before and after a crest maximum event as well as crest surface water velocity. The movement of a single heated patch on a C3N7 breaking wave is presented in figure 3. The location of the crest maximum is at the centre of the image. The first image shows the heated patch just before the breaking onset. Images (b) and (c) present the patch 33.33 ms and 66.66 ms thereafter. By digitising the front of the patches in successive frames and having the time between each frame, the water surface velocities could be calculated.

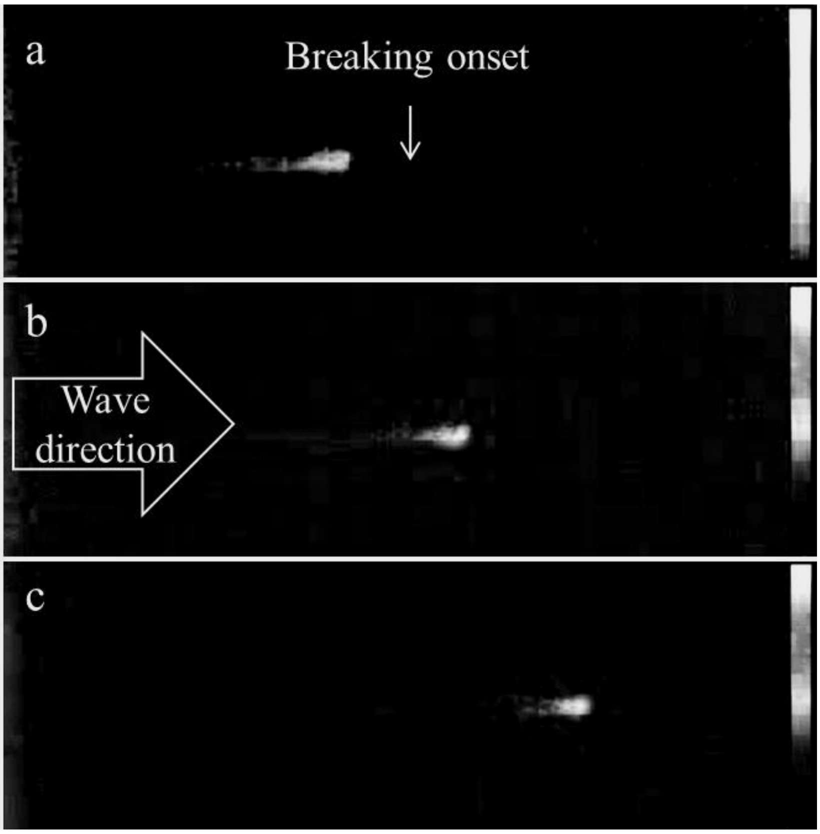

Figure 3. A heated patch generated by the CO_2 laser on a C3N7 wave packet (a) before the breaking onset, (b) and (c) on the breaking wave. The time between each frame is 33.33 ms.

After measuring the fluid velocities at the wave surface during the transit of a crest maximum event, these velocities could be interpolated in time to obtain a velocity at the crest that was immediately local in space to the crest maximum location. A polynomial curve was fitted to a sequence of such measurements (figure 4) to interpolate in space to obtain a single measurement of velocity at the crest group maximum. This entire sequence was repeated 7–10 times to quantify measurement repeatability. In each case, it was found that the water surface wave particle velocity increases to a maximum at the crest. The surface velocity for a marginal breaking C3N7 and C2N5 wave groups with the polynomial curve fitted to the velocities are illustrated in figure 4a. Distance in this figure indicates location relative to the crest maximum. As shown, the maximum water velocity occurs at a crest maximum event.

Further, the wave crest speeds were measured during transit of a crest maximum event. In contrast with surface velocity, the wave crest itself systematically slows down to a minimum speed at the crest maximum. The result of the crest speed measurement for the C3N7 wave group case shown in figure 3 and C2N5 wave groups with the polynomial curve fitted to the speeds are presented in figure 4b.

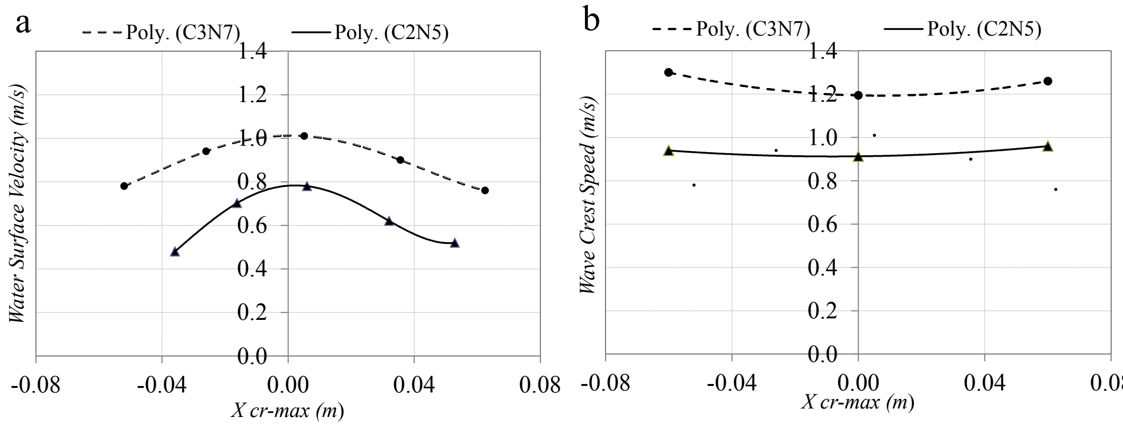

Figure 4. (a) Surface water particle velocities (m/s) and (b) wave crest speeds (m/s) in the vicinity of the crest maximum for marginal breaking C3N7 (dashed curve) and C2N5 (solid curve) wave groups. Horizontal axis is the distance relative to the location of crest maximum (m).

5. Summary and conclusions

In the present study a thermal image velocimetry technique using infrared imagery was developed to measure the water surface velocity. Heated droplets and a CO_2 laser were used to generate heated patches on the water surface. Unidirectional deep-water waves were generated in a 2D wind wave flume. Three wave types, i.e. monochromatic waves, bimodal spectrum (Class 2) and chirped wave packet (Class 3), were used for evaluation of wave breaking criteria.

It was shown that the TIV technique using heated water droplets can quantify the surface velocity for monochromatic, non-breaking waves without wind forcing.

A CO_2 laser system was developed to irradiate the water surface so as to improve the localisation of hot spot formation on the water surface. With this enhancement, the TIV technique can capture crest water velocities for unforced and wind-forced grouped waves.

These results show that the surface fluid velocity increases to a maximum at the crest maxima. At the same time, the wave profile crest speeds take on their minimum values at the crest maxima. The present results show that at the crest maximum location, the ratio of the water velocity U_s at the crest maximum to the wave profile speed C for marginal breaking waves is consistently less than unity.

References

[1] Peirson W L 1997 *Exp. Fluids* **23** 427
[2] Gray C and Greated C A 1998 *Opt. Lasers Eng.* **9** 265
[3] Siddiqui M H K *et al* 2001 *Phys. Fluids* **13** 1891
[4] Jensen A *et al* 2001 *Exp. Fluids* **30** 500
[5] Jessup A T and Phadnis K R 2005 *Meas. Sci. Technol.* **16** 1961
[6] Muste M *et al* 2005 *Flow Meas. Instru.* **16** 47
[7] Garbe C S *et al* 2007 *Transport at the Air–Sea Interface* eds Garbe C S *et al* (Heidelberg: Springer) 223-39
[8] Jessup A T *et al* 1997 *Nature* **385** 52
[9] Banner M L and Peirson W L 1998 *J. Fluid Mech.* **364** 115
[10] Zappa C J *et al* 2001 *J. Geophys. Res.* **106** 9385
[11] Stansell P and Macfarlane C 2002 *J. Phys. Oceanogr.* **32** 1269
[12] Peirson W L and Banner M L 2003 *J. Fluid Mech.* **479** 1
[13] Peirson W L *et al* 2014 *J. Fluid Mech.* **743** 399
[14] Banner M L *et al* 2014 *Phys. Rev. Lett.*, **112** 114502
[15] Barthelemy X *et al* 2015 *J. Fluid Mech.* under review
[16] Banner M L and Peirson W L 2007 *J. Fluid Mech.* **58**5 93